Natural Resources for Human Health
eISSN: 2583-1194

Original Research

Received 23 May 2026
Revised 25 June 2026
Accepted 18 July 2026

Natural Resources for Human Health 2026, Vol. 6(8s): 1608–1626

KEYWORDS:
Slag, Slag Sand, Mechanical Properties, Taguchi, Anova, XRD, and SEM

A Study on Mechanical Properties of Partially Replaced Slag and Slag Sand to OPC and M-Sand in Concrete

Deepak[1], Dr. H. C. Chowdegowda[2], Dr. Nakul N[3], Nandini N Murthy[4]

[1]Research Scholar, [2]Associate Professor
[1]Research Scholar, Department of Civil Engineering, P.E.S. College of Engineering, MANDY- 571 401, Affiliated to Visvesvaraya Technological University (VTU), BELGAUM – 590 018
[2]Associate Professor and Head, Department of Civil Engineering, P.E.S. College of Engineering, MANDY- 571 401
[3]Vice-Principal and Associate Professor, Department of Civil Engineering, Mysuru Royal Institute of Technology, MANDYA – 571 606
[4]Secretory, Mysuru Royal Education Trust, MANDYA – 571 606

ABSTRACT: Concrete production contributes significantly to carbon emissions and natural resource depletion due to the extensive use of cement and river sand. This study investigates the combined use of Ground Granulated Blast Furnace Slag (GGBFS) as a partial cement replacement and slag sand as a fine aggregate replacement in M40 grade concrete. A Taguchi L16 orthogonal array was employed to optimize GGBFS content (10–40%), slag sand replacement (10–40%), superplasticizer dosage, and curing age (7–90 days), while ANOVA identified the significance of each factor. The optimum mix, containing 10% GGBFS, 40% slag sand, and 2% superplasticizer cured for 90 days, achieved compressive, split tensile, and flexural strengths of 44.61 MPa, 4.21 MPa, and 4.31 MPa, respectively. XRD and SEM analyses confirmed enhanced C-S-H formation and a denser microstructure. Optimized mix reduced cement consumption by 10% and natural sand usage by 40%, demonstrating a sustainable, durable, & high-performance concrete suitable for construction applications.

1. INTRODUCTION

The utilization of industrial by-products in concrete production has gained significant attention due to increasing environmental concerns associated with cement manufacturing and depletion of natural resources. Steel slag and Ground Granulated Blast Furnace Slag (GGBS) have emerged as promising sustainable materials owing to their cementitious and pozzolanic characteristics. Early investigations established that steel slag possesses favorable physical and chemical properties that make it suitable for use in cementitious systems and construction applications [1].

The hydration behavior of steel slag has been extensively studied, revealing that its cementitious activity contributes to strength development and long-term performance of concrete. Improvements in hydration characteristics have been achieved through modification of mineral compositions and processing techniques, resulting in enhanced reactivity and greater utilization efficiency [2,3]. The incorporation of steel slag has also been reported to influence the fresh properties of concrete, particularly workability, due to its rough texture and water absorption characteristics [4].

Research on the use of steel slag as aggregate has demonstrated its effectiveness in improving mechanical performance and durability. Enhanced stability, abrasion resistance, and structural integrity have been observed when steel slag is utilized as coarse or fine aggregate in construction materials [5–10]. The use of steel-making slag as a partial replacement for cement has further shown improvements in compressive strength and hydration processes through the formation of additional cementitious products [11].

Several studies have focused on improving the hydration activity and pozzolanic behavior of steel slag. The findings indicate that reducing particle size and optimizing mineralogical composition significantly enhance its reactivity and contribution to strength development [12,13]. Furthermore, steel slag has been successfully incorporated into clinker production and blended cement systems, offering both environmental and economic advantages while maintaining satisfactory engineering performance [14–16].

Among supplementary cementitious materials, GGBS has received widespread acceptance due to its ability to improve long-term strength, durability, and sustainability of concrete. Experimental investigations have shown that appropriate replacement levels of cement with GGBS enhance compressive strength through continued hydration and pozzolanic reactions [17]. The incorporation of GGBS has also been found to reduce bleeding, improve cohesiveness, and contribute to the development of a denser microstructure [18,19].

The efficiency of GGBS as a cement replacement material has been validated through various performance assessments. Significant improvements in compressive strength, permeability resistance, and durability characteristics have been reported when GGBS is incorporated into concrete mixtures [20,21]. Enhanced resistance to aggressive environmental conditions and reduced pore connectivity have also been observed, leading to improved long-term durability [22–24].

Further investigations have highlighted the synergistic interaction between steel slag and blast furnace slag in cementitious systems. The combined utilization of these materials has been shown to accelerate hydration reactions, improve microstructural development, and increase strength performance compared to conventional mixtures [25]. The formation of additional calcium silicate hydrate (C-S-H) gel and the refinement of pore structure contribute significantly to these improvements[26-28].

Although substantial research has been conducted on the individual utilization of steel slag and GGBS, studies investigating their simultaneous incorporation as replacements for both cement and fine aggregate remain limited[29-32]. Most previous investigations have focused on either mechanical performance or durability characteristics, while comprehensive optimization approaches are comparatively scarce. Furthermore, limited attention has been given to the application of statistical optimization techniques such as the Taguchi method and ANOVA for determining optimum replacement levels[33-38]. Therefore, a detailed investigation on the combined utilization of GGBS and slag sand in concrete, supported by mechanical, durability, and microstructural analyses, is required to establish an optimized and sustainable concrete mixture.

2. OBJECTIVES OF THE PRESENT STUDY

- To investigate the effect of partial replacement of OPC with GGBFS and M-sand with GBFSS on the mechanical properties of M40 grade concrete.
- To optimize slag content, slag sand content, superplasticizer dosage, and curing age using the Taguchi L16 design methodology.
- To evaluate compressive strength, split tensile strength, and flexural strength of the developed concrete mixes.
- To determine the statistical significance and contribution of individual parameters using ANOVA.
- To identify the hydration products and crystalline phases present in the optimized concrete mixes using X-Ray Diffraction (XRD) & Scanning Electron Microscopy (SEM) analysis and correlate them with the controlled mix.

3. MATERIALS AND METHODS

Concrete mixes were prepared using OPC 43 Grade cement of Coromandel International, M-sand, 20 mm coarse aggregate, potable water, and Ground Granulated Blast Furnace Slag (GGBFS) with Granulated Blast Furnace Slag Sand (GBFSS) procured from Quality Polytech. Mix design was carried out as per IS 10262:2019.

The experimental program was developed using the Taguchi-based DOE approach by considering compressive strength as the primary response with a “larger-the-better” S/N ratio criterion. Orthogonal array design, factor definition, analysis, and optimization were performed using Minitab. Concrete cubes, cylinders, and beams were cast with varying replacement levels of GGBFS and GBFSS and tested for compressive, split tensile, and flexural strengths in accordance with IS 516:1959 and IS 5816:1999. S/N ratio analysis, mean plots, ANOVA, and confirmation tests were carried out to determine the optimum sustainable mix proportion with improved mechanical performance.

Table 3.1. Detailed Mix Proportions for Taguchi L16 Experimental Design (per m³ of Concrete)

Mix No.	GGBFS (%)	Slag Sand (%)	SP (%)	Cement (kg)	GGBFS (kg)	M-Sand (kg)	Slag Sand (kg)	Coarse Aggregate (kg)	Water (L)
L1	10	10	0.5	394.2	43.8	639.0	71.0	1175	197
L2	10	20	1.0	394.2	43.8	568.0	142.0	1175	197
L3	10	30	1.5	394.2	43.8	497.0	213.0	1175	197
L4	10	40	2.0	394.2	43.8	426.0	284.0	1175	197
L5	20	10	1.0	350.4	87.6	639.0	71.0	1175	197
L6	20	20	0.5	350.4	87.6	568.0	142.0	1175	197
L7	20	40	2.0	350.4	87.6	426.0	284.0	1175	197
L8	20	30	1.5	350.4	87.6	497.0	213.0	1175	197
L9	30	10	1.5	306.6	131.4	639.0	71.0	1175	197
L10	30	20	2.0	306.6	131.4	568.0	142.0	1175	197
L11	30	30	0.5	306.6	131.4	497.0	213.0	1175	197
L12	30	40	1.0	306.6	131.4	426.0	284.0	1175	197
L13	40	10	2.0	262.8	175.2	639.0	71.0	1175	197
L14	40	20	1.5	262.8	175.2	568.0	142.0	1175	197
L15	40	30	1.0	262.8	175.2	497.0	213.0	1175	197
L16	40	40	0.5	262.8	175.2	426.0	284.0	1175	197

The mix proportions for all experimental combinations were developed based on the control M40 concrete mix designed in accordance with IS 10262:2019. Cement was partially replaced by GGBFS at levels of 10%, 20%, 30%, and 40%, while M-sand was replaced by slag sand at levels of 10%, 20%, 30%, and 40%. Superplasticizer dosage was varied between 0.5% and 2.0% by weight of binder. The detailed quantities of constituent materials used for each Taguchi L16 experimental run are presented in Table 3.1. This detailed presentation improves the reproducibility of the experimental program and facilitates future comparative studies.

4. RESULTS AND DISCUSSION

a. Basic properties

The materials used in concrete specimens were having equally diverse properties and behaviour. The properties of materials were determined in the laboratory as per standard specifications and represented in Table 4.1.1.

The specific gravity of fine aggregates, cement and GGBFS are within the specified limits. Standard consistency and Fineness of cement and GGBFS confirms to BIS. Initial setting time and final setting time of cement is within the specified limits whereas, GGBFS exceeded the threshold due to lack of calcium chloride content. Fineness Modulus, Water absorption and % air voids of fine aggregates were as per the specifications.

Table 4.1.1.: Basic test results of R-Sand, M-Sand, GGBFSS, Cement and GGBFS

Property	Cement	Slag	Types of Fine Aggregates			Threshold Value
			M-sand	Slag Sand	Coarse Aggregate	
Specific gravity	3.10	3.24	2.64	2.61	2.76	Fine Aggregate: 2.6-2.8
Standard consistency in %	32.3	30.3	-	-	-	26-33
Initial setting time in min.	28	38	-	-	-	30 (Minimum)
Final setting time in min.	410	608	-	-	-	600 (Maximum)
Fineness in %	5.4	5.2	-	-	-	<10
Fineness Modulus	-	-	2.81	2.7	-	Fine sand: 2.2-2.6 Medium sand: 2.6-2.9 Coarse sand: 2.9-3.2
Water absorption in %	-	-	0.38	0.56	0.63	Coarse aggregate: <1.4 Fine Aggregate:<2
Bulk density, in g/cc	-	-	1.43	1.4	-	-
% Air voids	-	-	2.71	2.9	-	-

Cement (SG 3.10) and slag (SG 3.24) are denser than aggregates, while M-sand (2.64) and slag sand (2.61) lie within the fine-aggregate range (2.6–2.8). Cement and slag meet BIS limits for standard consistency (32.3%, 30.3%) and fineness (<10%). Setting times are generally acceptable: cement's final setting (410 min) is within limits though its initial setting (28 min) is 2 min below the stated minimum; slag's final setting (608 min) slightly exceeds the 600 min limit, indicating slower setting. Sand properties—fineness modulus (2.7–2.81), water absorption (0.38–0.56%), bulk density (~1.40–1.43 g/cc), and air voids (~2.7–2.9%)—all meet expected ranges.

4.2 Characteristics/Compositions of GGBFS

Table 4.2.1 represents the Characteristics/Compositions of GGBFS which confirms the IS 12089:1987 specifications.

Table 4.2.1: Characteristics/Compositions of GGBFS (Conforms IS 12089:1987)

Sl No.	Characteristics	Requirements as Per IS : 12089	Test Results
1	SiO_2 (%)	-	33.30
2	Al_2O_3 (%)	-	21.74
3	Fe_20_3 (%)	-	0.80
4	Cao (%)	-	34.50
5	Mgo (%)	17.0 (Max)	8.30
6	Loss on Ignition (%)	-	0.33
7	IR (%)	5.0 (Max)	0.31
8	Manganese Content (%)	5.5 (Max)	0.09

9	Sulphide Sulphur (%)	2.0 (Max)	0.45
10	Glass Content (%)	85 (Min)	90
11	Moisture Content (%)	-	11.74
12	Particle Size Passing 50.0 mm	95%	100%
13	Chemical Mouli (CaO + MgO + Al_2O_3)/ SiO_2	Greater than or equals to 1.0	1.93

The slag's chemical and physical tests meet IS:12089. Major oxides (SiO2 33.3%, Al2O3 21.7%, CaO 34.5%) are typical for GGBFS, and MgO (8.3%), LOI (0.33%), IR (0.31%), Mn (0.09%) and sulphide-S (0.45%) are within specified limits. Glass content is high (90% > 85% min) and particle size is acceptable (100% passing 50 mm). The chemical modulus (CaO+MgO+Al2O3)/SiO2=1.93(CaO+MgO+Al2O3)/SiO2=1.93 exceeds the required 1.0, indicating good basicity and reactivity. One operational note: moisture content is 11.74% and should be controlled or reduced before use.

5. RESULTS AND DISCUSSIONS

5.1 Mechanical Properties of M40 Grade Concrete

5.1.1 Compressive Strength of M40

Table 5.1.1: Compressive Strength of M40, L16 Array

Sl No	Slag	Slag Sand	Super Plasticizer (%)	Curing Age	Compressive Strength (N/mm²)	SNRA1	FITS
1	10	10	0.5	7	30.11	29.57422	34.99172
2	10	20	1	28	41.22	32.30216	38.47598
3	10	30	1.5	56	43.59	32.78774	42.89097
4	10	40	2	90	45.01	33.06618	48.10373
5	20	10	1	56	43.14	32.6976	40.41327
6	20	20	0.5	90	42.95	32.65926	44.32648
7	20	30	2	7	33.7	30.5526	35.28242
8	20	40	1.5	28	42.711	32.61079	37.46713
9	30	10	1.5	90	43.76	32.82155	43.84043
10	30	20	2	56	41.6	32.38187	40.01187
11	30	30	0.5	28	40.22	32.08884	34.38198
12	30	40	1	7	28.51	29.09994	32.28192
13	40	10	2	28	38.05	31.60709	34.50338
14	40	20	1.5	7	25.61	28.16819	31.10377
15	40	30	1	90	37.72	31.53143	41.53203
16	40	40	0.5	56	38.11	31.62078	36.40392

The compressive strength test of M40 grade concrete was determined with the L16 array of Taguchi design. The replacement levels of Slag, Slag Sand, and Super plasticizer with the different curing age were considered. The compressive strength of such combinations were represented in the Table 5.1.1. The L4, i.e. 10% Slag, 40% Slag Sand, 2% super plasticizer with 90 days curing resulted highest compressive strength (33.06N/mm²).

5.1.1.1 Analysis of Variance and Main effects plot of SN Ratios for Compressive Strength (M40)

Table 5.1.1.1: Analysis of Variance of SN Ratios for Compressive Strength (M40)

Source	DF	Seq SS	Adj SS	Adj MS	F	P(e^{-21})
Slag	3	4.5808	4.5808	1.52694	16.66	0.022
Slag Sand	3	0.2985	0.2985	0.09948	1.09	0.474
Super Plasticizer (%)	3	0.5646	0.5646	0.18820	2.05	0.285
Curing Age	3	27.2591	27.2591	9.08636	99.14	0.002
Residual Error	3	0.2750	0.2750	0.09165	-	-
Total	15	32.9779	-	-	-	-

The Table 5.1.1.1 represents the Anova Test (Ho 5.5.1 vs Ha 5.5.1) for Compressive Strength Result of Partially replaced Slag Sand and Slag to M-Sand and OPC. It can be observed that the P-values of Slag, Slag Sand, Super plasticizer, and cuing age are $0.022e^{-21}$, $0.474e^{-21}$, $0.285e^{-21}$ and $0.002e^{-21}$.

The hypothesis considered was Ho 5.1.1.1 and Ha 5.1.1.1 is as follows

- **Ho 5.1.1.1:** There is no significant variation amongst the compressive strength of % replaced Slag Sand and Slag to M-Sand and OPC for 5 different curing ages
- **Ha 5.1.1.1:** There is a significant variation amongst the compressive strength of % replaced Slag Sand and Slag to M-Sand and OPC for 5 different curing ages

From the ANOVA test results of Table 5.1.1.1 it is observed that the P-value is <0.05 i.e. Significance Level, so reject the null hypothesis (Ho 5.1.1.1) and accept the alternate hypothesis (Ha 5.1.1.1).

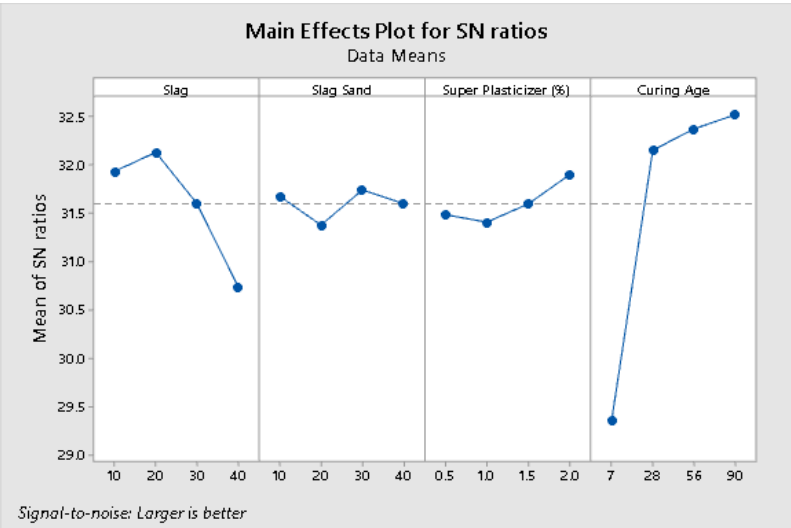

Figure 5.1.1.1: Main effects plot of SN ratios for Compressive Strength (M40)

From the main effect plot for the factors affecting the compressive strength are shown in the figure 5.1.1.1, The factor with the largest differences between its highest and lowest average SN ratio had influenced most on the response. The Slag having largest difference between the heights and slag sand had lowest SN ratio which influenced most on the response.

5.1.1.2: Response and Residual Plots of SN Ratios for Compressive Strength (M40)

Table 5.1.1.2: Response of SN Ratios (Larger is better) for Compressive Strength (M40)

Level	Slag	Slag Sand	Super Plasticizer (%)	Curing Age
1	31.93	31.68	31.49	29.35
2	32.13	31.38	31.41	32.15
3	31.60	31.74	31.60	32.37
4	30.73	31.60	31.90	32.52
Delta	1.40	0.36	0.49	3.17
Rank	2	4	3	1

The delta statistic, highest and lowest mean delta factor was 3.17 and 0.36. The most affected material's rank order observed was first Curing Age, second Slag, third Super plasticizer, and fourth Slag Sand.

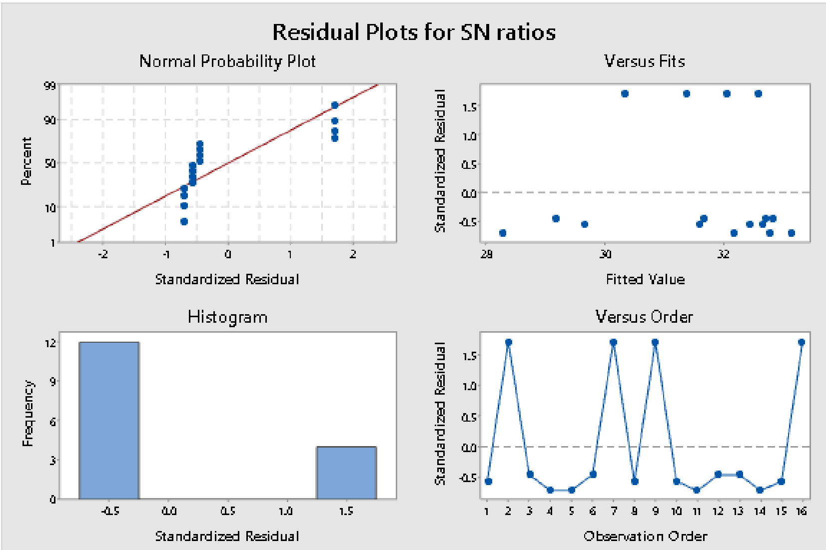

Figure 5.1.1.2: Residual Plots for SN ratios for Compressive Strength (M40)

The residual analysis indicates that the model assumptions are reasonably satisfied, as most residuals follow the normal probability line, confirming approximate normality. Slight deviations and left skewness in the residual plots suggest minor non-linearity and heteroscedasticity. The residuals versus observation order plot shows small cyclic variations, indicating possible autocorrelation or systematic experimental variation. Overall, the model shows acceptable adequacy with minor deviations.

5.1.1.3: Compressive Strength Comparison of M40 with Conventional Concrete

Table 5.1.1.3: Compressive Strength Comparison of M40 with Conventional Concrete

Compressive Strength (N/mm²)				
Grade of Concrete	**7 Day**	**28 Day**	**56 Day**	**90 Day**
CM (M40)	27.11	39.8	40.91	43.57
L4 (M40)	28.67	40.77	42.55	44.61

The compressive strength results indicate that both CM and L4 mixes gained strength with increase in curing age. The control mix (CM) achieved compressive strengths of 27.11 N/mm², 39.8 N/mm², 40.91 N/mm², and 43.57 N/mm² at 7, 28, 56, and 90 days respectively. In comparison, the L4 mix exhibited higher strength values at all curing periods, recording 28.67 N/mm² at 7 days, 40.77 N/mm² at 28 days, 42.55 N/mm² at 56 days, and 44.61 N/mm² at 90 days.

5.1.2 Split Tensile Strength Analysis of M40

Table 5.1.2: Split Tensile Strength of M40, L16 Array

Sl No	Slag	Slag Sand	Super Plasticizer (%)	Curing Age	Split Tensile Strength (N/mm²)	SNRA1	FITS
1	10	10	0.5	7	2.96	9.425834	3.510011
2	10	20	1	28	4.33	12.72976	3.845328
3	10	30	1.5	56	4.52	13.10277	4.283585
4	10	40	2	90	4.68	13.40492	4.810076
5	20	10	1	56	4.41	12.88877	4.289085
6	20	20	0.5	90	4.57	13.19832	4.663076
7	20	30	2	7	3.26	10.26435	3.621511
8	20	40	1.5	28	3.93	11.88785	3.804328
9	30	10	1.5	90	4.68	13.40492	4.847576
10	30	20	2	56	4.57	13.19832	4.374085
11	30	30	0.5	28	4.24	12.54732	3.683828
12	30	40	1	7	3.11	9.855208	3.401511
13	40	10	2	28	4.25	12.56778	3.994328
14	40	20	1.5	7	3.44	10.73117	3.559511
15	40	30	1	90	4.31	12.68955	4.654076
16	40	40	0.5	56	4.11	12.27684	4.028085

The Split tensile strength test of M40 grade concrete was determined with the L16 array of Taguchi design. The replacement levels of Slag, Slag Sand, and Super plasticizer with the different curing age were considered. The Split tensile strength of such combinations was represented in the Table 5.1.2. The L4, i.e. 10% Slag, 40% Slag Sand, 2% super plasticizer with 90 days curing had resulted highest Split tensile strength (13.40 N/mm²).

5.1.2.1 Analysis of Variance and Main effects plot of SN Ratios for Split Tensile Strength (M40)

Table 5.1.2.1: Analysis of Variance for SN Ratios of Split Tensile Strength (M40)

Source	DF	Seq SS	Adj SS	Adj MS	F	$P(e^{-21})$
Slag	3	0.0995	0.0995	0.03316	0.14	0.932
Slag Sand	3	0.7619	0.7619	0.25396	1.05	0.485
Super Plasticizer (%)	3	0.6199	0.6199	0.20663	0.85	0.551
Curing Age	3	23.8897	23.8897	7.96325	32.85	0.009

Residual Error	3	0.7273	0.7273	0.24243	-	-
Total	15	26.0983	-	-	-	-

The Table 5.1.2.1 represents the Anova Test (Ho 5.1.2.1 vs Ha 5.1.2.1) for Split Tensile Strength Result of Partially replaced Slag Sand and Slag to M-Sand and OPC. It can be observed that the P-values of Slag, Slag Sand, Super plasticizer, and cuing age are $0.932e^{-21}$, $0.485e^{-21}$, $0.551e^{-21}$ and $0.009e^{-21}$.

The hypothesis considered was Ho 5.1.2.1 and Ha 5.1.2.1 is as follows

- **Ho 5.1.2.1:** There is no significant variation amongst the Split tensile strength of % replaced Slag Sand and Slag to M-Sand and OPC for 5 different curing ages
- **Ha 5.1.2.1:** There is a significant variation amongst the Split tensile strength of % replaced Slag Sand and Slag to M-Sand and OPC for 5 different curing ages

From the ANOVA test results of Table 5.1.2.1 it is observed that the P-value is <0.05 i.e. Significance Level, so reject the null hypothesis (Ho 5.1.2.1) and accept the alternate hypothesis (Ha 5.1.2.1).

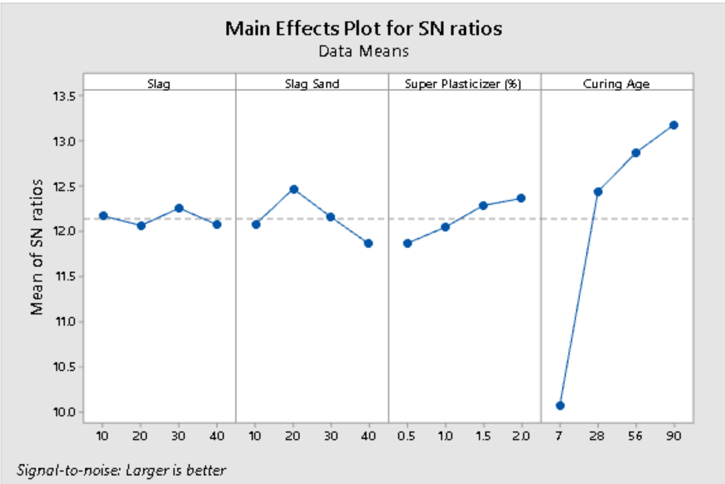

Figure 5.1.2.1: Main effects plot for SN ratios for Split Tensile Strength (M40)

From the main effect plot for the factors affecting the Split tensile strength are shown in the figure 5.1.2.1, The factor with the largest differences between its highest and lowest average SN ratio had influenced most on the response. The Slag having largest difference between the heights and slag sand had lowest SN ratio which influenced most on the response.

5.1.2.2: Response and Residual Plots of SN Ratios for Split Tensile Strength (M40)

Table 5.1.2.2: Response Table for SN Ratios (Larger is better) Split Tensile Strength (M40)

Level	**Slag**	**Slag Sand**	**Super Plasticizer (%)**	**Curing Age**
1	12.17	12.07	11.86	10.07
2	12.06	12.46	12.04	12.43
3	12.25	12.15	12.28	12.87
4	12.07	11.86	12.36	13.17
Delta	0.19	0.61	0.50	3.11
Rank	4	2	3	1

The delta statistic, highest and lowest mean delta factor was 3.11 and 0.19. The most affected material's rank order observed was first Curing Days, second Slag Sand, third Super plasticizer, and fourth Slag.

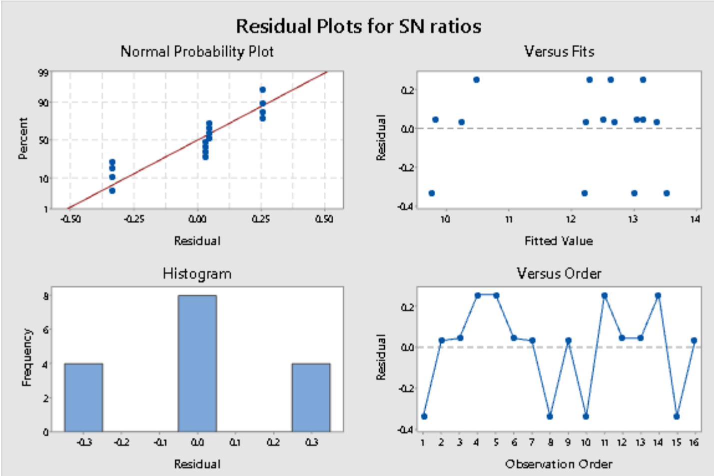

Figure 5.1.2.2: Residual Plots for SN ratios for Flexural Strength (M40)

The residual analysis confirms that the model assumptions are reasonably satisfied. The residuals are approximately normally distributed and uniformly scattered, indicating good model adequacy and constant variance. Minor skewness and slight cyclic variation were observed, but no significant autocorrelation or non-linearity was identified. Overall, the model is considered reliable and statistically acceptable.

5.1.2.3: Split Tensile Strength Comparison of M40 with Conventional Concrete

Table 5.1.2.3: Split Tensile Strength Comparison of M40 with Conventional Concrete

Split Tensile Strength (N/mm²)				
Grade of Concrete	**7 Day**	**28 Day**	**56 Day**	**90 Day**
CM	2.55	3.42	3.81	4.17
M40	2.61	3.66	3.97	4.21

The split tensile strength of both CM and M40 concrete increased with curing age. The CM mix achieved strengths of 2.55, 3.42, 3.81, and 4.17 N/mm² at 7, 28, 56, and 90 days respectively, whereas the M40 mix showed higher values of 2.61, 3.66, 3.97, and 4.21 N/mm². The results indicate that the modified M40 concrete exhibited better tensile performance than conventional concrete due to improved bonding and denser microstructure.

5.1.3 Flexural Strength Analysis of M40

Table 5.1.3: Flexural Strength Analysis of M40, L16 Array

Sl No	Slag	Slag Sand	Super Plasticizer (%)	Curing Age	Flexural Strength (N/mm²)	SNRA1	FITS
1	10	10	0.5	7	3.21	10.1301	3.788014
2	10	20	1	28	4.79	13.60671	4.17881
3	10	30	1.5	56	4.79	13.60671	4.657538
4	10	40	2	90	4.86	13.73273	5.211637
5	20	10	1	56	4.66	13.36772	4.385538

eISSN: 2583-1194

6	20	20	0.5	90	4.41	12.88877	4.778637
7	20	30	2	7	3.88	11.77663	4.024014
8	20	40	1.5	28	4.53	13.12196	4.25381
9	30	10	1.5	90	4.7	13.44196	4.794637
10	30	20	2	56	4.78	13.58856	4.494538
11	30	30	0.5	28	4.61	13.27402	3.94781
12	30	40	1	7	3.44	10.73117	3.811014
13	40	10	2	28	4.26	12.58819	3.99781
14	40	20	1.5	7	3.11	9.855208	3.700014
15	40	30	1	90	4.59	13.23625	4.708637
16	40	40	0.5	56	4.36	12.78973	4.247538

The Flexural Strength test of M40 grade concrete was determined with the L16 array of Taguchi design. The replacement levels of Slag, Slag Sand, and Super plasticizer with the different curing age were considered. The Flexural Strength of such combinations was represented in the Table 5.1.3. The L4, i.e. 10% Slag, 40% Slag Sand, 2% super plasticizer with 90 days curing had resulted highest Flexural Strength (13.73 N/mm^2).

5.1.3.1 Analysis of Variance and Main effects plot of SN Ratios for Flexural Strength (M40)

Table 5.1.3.1: Analysis of Variance for SN Ratios of Flexural Strength (M40)

Source	DF	Seq SS	Adj SS	Adj MS	F	P(e^{-21})
Slag	3	1.2886	1.2886	0.4295	2.65	0.223
Slag Sand	3	0.7999	0.7999	0.2666	1.64	0.347
Super Plasticizer (%)	3	0.9546	0.9546	0.3182	1.96	0.297
Curing Age	3	21.1103	21.1103	7.0368	43.36	0.006
Residual Error	3	0.4869	0.4869	0.1623	-	-
Total	15	24.6402	-	-	-	-

The Table 5.1.3.1 represents the Anova Test (Ho 5.1.3.1 vs Ha 5.1.3.1) for Flexural Strength Result of Partially replaced Slag Sand and Slag to M-Sand and OPC. It can be observed that the P-values of Slag, Slag Sand, Super plasticizer, and cuing age are $0.223e^{-21}$, $0.347e^{-21}$, $0.297e^{-21}$ and $0.006e^{-21}$.

The hypothesis considered was Ho 5.1.3.1 and Ha 5.1.3.1 as follows

- **Ho 5.1.3.1:** There is no significant variation amongst the Flexural Strength of % replaced Slag Sand and Slag to M-Sand and OPC for 5 different curing ages
- **Ha 5.1.3.1:** There is a significant variation amongst the Flexural Strength of % replaced Slag Sand and Slag to M-Sand and OPC for 5 different curing ages

From the ANOVA test results of Table 5.1.3.1 it is observed that the P-value is <0.05 i.e. Significance Level, so reject the null hypothesis (Ho 5.1.3.1) and accept the alternate hypothesis (Ha 5.188.3.1).

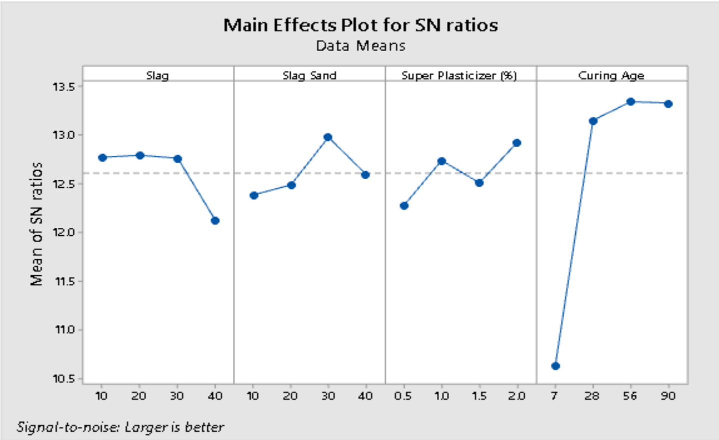

Figure 5.1.3.1: Main effects plot for SN ratios of Flexural Strength (M40)

From the main effect plot for the factors affecting the Flexural Strength are shown in the figure 5.1.3.1, The factor with the largest differences between its highest and lowest average SN ratio had influenced most on the response. The Curing Age having largest difference between the heights and slag sand had lowest SN ratio which influenced most on the response.

5.1.3.2: Response and Residual Plots of SN Ratios for Flexural Strength (M40)

Table 5.1.3.2: Response for SN Ratios (Larger is better) Flexural Strength (M40)

Level	**Slag**	**Slag Sand**	**Super Plasticizer (%)**	**Curing Age**
1	12.77	12.38	12.27	10.62
2	12.79	12.48	12.74	13.15
3	12.76	12.97	12.51	13.34
4	12.12	12.59	12.92	13.32
Delta	0.67	0.59	0.65	2.71
Rank	2	4	3	1

The delta statistic, highest and lowest mean delta factor was 2.71 and 0.59. The most affected material's rank order observed was first Curing Age, second Slag, third Super plasticizer, and fourth Slag Sand.

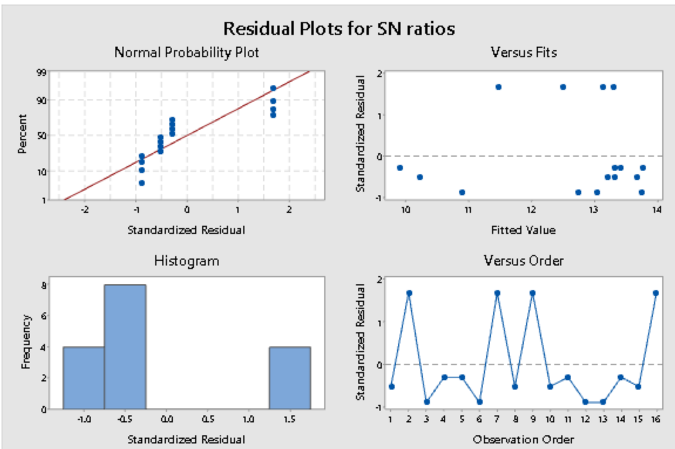

Figure 5.1.3.2: Residual Plots for SN ratios for Split Tensile Strength (M40)

The residual analysis indicates that the model assumptions are reasonably satisfied. The residuals are approximately normally distributed and uniformly scattered, confirming good model adequacy and homoscedasticity. Minor skewness and slight cyclic variation were observed, but no significant non-linearity, outliers, or autocorrelation were identified. Overall, the residual plots validate the reliability and statistical acceptability of the model.

5.1.3.3: Flexural Strength Comparison of M40 with Conventional Concrete

Table 5.1.3.3: Flexural Strength Comparison of M40 with Conventional Concrete

Flexural Strength (N/mm²)				
Grade of Concrete	**7 Day**	**28 Day**	**56 Day**	**90 Day**
CM	3.08	3.32	3.69	4.01
M40	3.21	3.41	3.83	4.31

The flexural strength of both CM and M40 concrete increased with curing age. The CM mix achieved flexural strengths of 3.08, 3.32, 3.69, and 4.01 N/mm² at 7, 28, 56, and 90 days respectively, whereas the M40 mix exhibited higher values of 3.21, 3.41, 3.83, and 4.31 N/mm². The results indicate that the modified M40 concrete showed better flexural performance than conventional concrete due to improved bonding characteristics and enhanced resistance to bending stresses.

5.1.4. XRD of M40 Controlled Mix Cured for 90Days

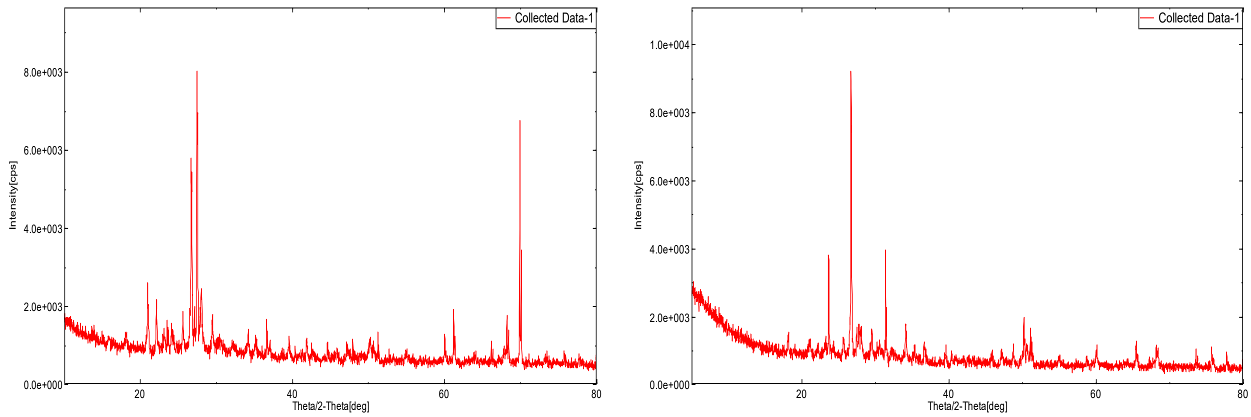

(A) **(B)**

Figure 5.1.4: XRD of M40 Controlled Mix (A) & M40 L4 Mix (B) Cured for 90Days

5.1.4: XRD Result's Comparison of Controlled Mix M40 with L4 Mix Cured for 90Days

The XRD results at 90 days show that the M40 L4 mix (10% Slag + 40% Slag Sand + 2% SP) exhibits superior hydration and microstructural development compared to the control M40 mix. The reduced portlandite (CH) peak indicates effective pozzolanic reactions, where slag materials consume CH and generate additional secondary C-S-H gel**.** The intensified C-S-H region confirms enhanced hydration and matrix densification. The presence of superplasticizer improves particle dispersion and reaction efficiency, resulting in fewer unreacted phases and a refined pore structure. Consequently, the L4 mix demonstrates improved durability, higher microstructural stability, and better long-term performance than conventional M40 concrete.

Table 5.1.4.1: XRD Result's Comparison of Controlled Mix with M40 L4 Mix Cured for 90Days

Parameter	Controlled M40 Mix (90 Days)	M40 L4 Mix (Slag 10%, Slag Sand 40%, SP 2%) (90 Days)
Main Peak (~28° 2θ)	Very strong, sharp peak (portlandite dominance)	Strong but slightly reduced; portlandite partially consumed via pozzolanic reaction
C-S-H Formation (18°–35° 2θ)	Present, but less intense	More pronounced; enhanced secondary C-S-H from slag reaction
Crystallinity	High; well-defined peaks	High, with more complex hydration products
Pozzolanic Reaction	Limited; high CH content remains	Strong; portlandite consumed to form more stable phases
Background Noise	Low to moderate; some unreacted phases present	Lower; indicates better hydration and matrix densification
Slag/Slag Sand Contribution	Not applicable	Active contributors to extended hydration and improved durability
SP (Superplasticizer) Role	Not present	Enhances particle dispersion, improves reaction kinetics
Residual Unreacted Phases	More likely, especially OPC-related	Fewer; better utilization of binder materials
Hydration Product Diversity	Mostly primary products (C-S-H, CH)	Primary + secondary (e.g., aluminosilicate hydrates from slag)
Long-Term Durability Potential	High, but limited by CH content	Very high; reduced CH, refined matrix, enhanced resistance to degradation

5.1.5. SEM of M40 Controlled Mix Cured for 90Days

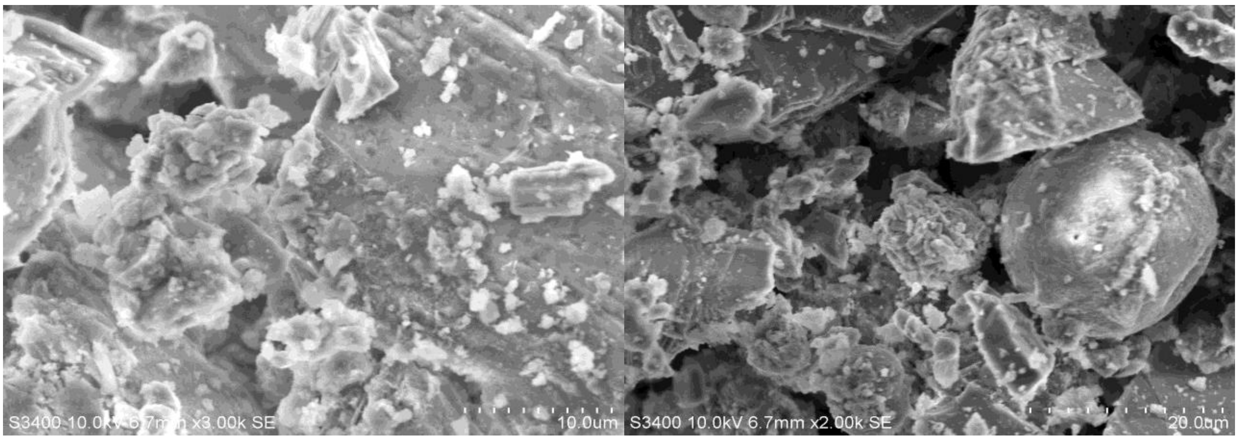

(A) (B)

Figure 5.1.5: SEM of Controlled Mix (A) & M40 L4 Mix Cured for 90Days

5.1.5.1. SEM Result's Comparison of Controlled Mix (A) & M40 L4 Mix Cured for 90Days

Table 5.1.5.1: SEM Result's Comparison of Controlled Mix (A) & M40 L4 Mix Cured for 90Days

Parameter / Feature	M40 Controlled Mix	M40 L4 Mix (10% Slag, 40% Slag Sand, SP 2%)	Remarks / Interpretation
Microstructure Density	Moderately dense with visible cracks and pores	Highly dense and compact with minimal visible pores	The L4 mix exhibits improved hydration and filler effects from slag and slag sand, leading to a denser, less porous matrix.
Calcium Hydroxide (CH)	Prominent flaky/plate-like CH crystals	Reduced CH due to pozzolanic activity of slag	Slag reacts with CH to form additional C-S-H gel, reducing free CH and enhancing durability.
C-S-H Gel Formation	Moderately developed, scattered	Extensive and continuous, fills voids	The L4 mix experiences enhanced hydration, with slag facilitating the formation of more C-S-H gel, leading to a stronger structure.
Unhydrated Cement Particles	Still present in small clusters	Very few unhydrated particles	Superplasticizer (SP) improves dispersion, while slag contributes to continued hydration, reducing unhydrated particles.
Void and Crack Presence	Visible micro-cracks and irregular voids	Greatly reduced; surface appears well-packed	The L4 mix has reduced porosity and fewer cracks, which leads to better durability and strength.
Surface Texture	Rough, angular particles and loosely bonded hydrates	Smoother, rounder particles and well-integrated hydrates	Slag and SP improve particle morphology, creating smoother, more uniform surfaces that promote better bonding.
Filler Effect	Minimal; relies on cement and natural sand	Significant due to fine slag sand particles	The L4 mix benefits from slag sand, which enhances packing density and reduces permeability.
Overall Microstructural Quality	Good (for high-grade concrete)	Excellent; optimized for strength and durability	The L4 mix shows superior microstructural performance, with improved hydration, reduced porosity, and enhanced durability compared to the controlled mix.

The SEM analysis reveals that the M40 L4 mix (10% Slag, 40% Slag Sand, and 2% SP**)** possesses a significantly denser and more compact microstructure than the control M40 concrete. The incorporation of slag and slag sand promotes additional C-S-H gel formation through pozzolanic reactions, reducing calcium hydroxide content and minimizing unhydrated particles. The L4 mix also exhibits fewer pores and microcracks, improved particle packing, and a more homogeneous matrix due to the filler effect of slag sand and enhanced dispersion provided by the superplasticizer. These microstructural improvements contribute to higher strength, lower permeability, and superior long-term durability compared to the conventional M40 mix.

CONCLUSION

- Specific gravity values of cement (3.10), slag (3.24), M-sand (2.64), slag sand (2.61), and coarse aggregate (2.76) were within permissible limits, confirming suitability for concrete production.
- Standard consistency of cement (32.3%) and slag (30.3%), along with fineness values of 5.4% and 5.2%, satisfied BIS specifications; slag showed higher setting times (38 min initial and 608 min final) compared to cement.
- M-sand (2.81) and slag sand (2.70) were classified as medium sand, while water absorption values of M-sand (0.38%), slag sand (0.56%), and coarse aggregate (0.63%) were within allowable limits.

- The optimized L4 mix (10% Slag, 40% Slag Sand, and 2% Super Plasticizer) exhibited higher compressive strength than conventional M40 concrete at all curing ages, achieving 44.61 N/mm² at 90 days compared to 43.57 N/mm² for CM.
- Early-age and later-age strength development of L4 was superior, with strengths of 28.67, 40.77, and 42.55 N/mm² at 7, 28, and 56 days respectively, indicating improved hydration and denser concrete microstructure.
- The modified M40 concrete exhibited higher split tensile strength than conventional concrete at all curing ages, achieving 2.61, 3.66, 3.97, and 4.21 N/mm² at 7, 28, 56, and 90 days respectively, compared to 2.55, 3.42, 3.81, and 4.17 N/mm² for CM.
- The optimum mix (10% Slag, 40% Slag Sand, and 2% Super Plasticizer) produced the highest split tensile strength, indicating improved bonding and crack resistance due to the filler effect and enhanced microstructure. The modified M40 concrete exhibited higher flexural strength than conventional concrete at all curing ages, achieving 3.21, 3.41, 3.83, and 4.31 N/mm² at 7, 28, 56, and 90 days respectively, compared to 3.08, 3.32, 3.69, and 4.01 N/mm² for CM.
- The optimum mix containing 10% Slag, 40% Slag Sand, and 2% Super Plasticizer achieved the highest flexural strength, indicating improved bonding characteristics and enhanced resistance to bending stresses.
- ANOVA and SN ratio analysis confirmed that curing age was the most significant factor influencing flexural strength, while slag and super plasticizer also contributed to improved performance compared to conventional concrete.
- The XRD results indicate that the M40 L4 mix (10% GGBFS, 40% slag sand, and 2% SP) developed a denser and more refined microstructure than the control mix due to enhanced pozzolanic activity and increased secondary C-S-H formation. The reduced portlandite content and improved hydration products suggest superior long-term strength and durability performance
- The SEM results show that the M40 L4 mix developed a denser and more homogeneous microstructure than the control mix due to enhanced C-S-H gel formation and reduced calcium hydroxide content. The lower porosity, fewer micro-cracks, and improved particle packing indicate superior strength and durability performance at later ages

REFERENCES

[1] Hafsi, H., Handel, N., Alshaikh, I.M.H., Aguiar, J., & Meftah, N. (2026). *Synergistic multiscale reinforcement of sand concrete incorporating steel fibers and granulated blast-furnace slag*. Scientific Reports, 16, Article 48446.

[2] Sobuz, M.H.R., Majumder, S., Afrin, S., Alzlfawi, A., Kabbo, M.K.I., Jameel, M., & Abubakar, S.A. (2026). *Evaluating the predictive accuracy of supervised machine learning models to explore the mechanical strength of blast furnace slag incorporated concrete*. Scientific Reports, 16, 6712.

[3] Baikerikar, A.V., Mohammed, B.S., & Singh, P. (2026). *Internal carbonation and performance optimization of slag concrete using carbonated water and graphene oxide: An RSM-based environmental assessment approach*. Diamond and Related Materials, 166, 113704.

[4] Prasad, N.S.S., Andal, M., Thatikonda, N., & Dubey, S. (2026). *Performance and microstructural insights of ambient-cured geopolymer concrete incorporating fly ash–GGBS binders and over-burnt brick aggregate*. Progress in Engineering Science, 3(2), 100288.

[5] Wang, L., Mou, L., Jia, J., Wan, Z., Meng, Z., & Zhou, X. (2026). *Study on multi-solid waste alkali-activated material concrete via RSM*. Buildings, 16(1), 198.

[6] Chaitanya, B.K., Madhavi, Y., Venkatesh, C., Durga, C.S.S., & Mitikie, B.B. (2026). *Multi-scale performance, life-cycle and economic assessment of blended concrete using recycled coarse aggregates*. Scientific Reports, 16, 13391.

[7] Deepti, Y., Kumar, S., Bandyopadhyay, A., Chithambaram, S.J., Kumar, P., & Sembeta, R.Y. (2026). *Synergic utilization of waste glass powder for fire-resilient and low alkali-activated concrete*. Scientific Reports, 16, 4989.

[8] Anonymous. (2026). *Experimental evaluation of fresh, mechanical, durability-related and microstructural properties of concrete incorporating GGBS and EAF slag aggregate*. Results in Engineering, 110165.

[9] Anonymous. (2026). *Thermal resistance of slag-blended concrete: Compressive strength, abrasion behaviour and microstructural changes*. European Journal of Environmental and Civil Engineering.

[10] Anonymous. (2026). *Experimental and RSM-based multi-objective optimization of low-carbon high-performance concrete incorporating silica fume and slag*. Cleaner Engineering and Technology, 32, 101233.

[11] Baikerikar, A.V., Fadhllurrohman, N.A., Mohammed, B.S., Tambusay, A., Suprobo, P., Sutrisno, W., & Irawan, C. (2025). *Synergistic effects of fly ash, ground granulated blast furnace slag, and graphene oxide in low-carbon concrete: Modelling, optimization, and sustainability assessment*. Scientific Reports.

[12] Insight into the durability of concrete based on ultrafine ground granulated blast furnace slag, phosphogypsum, and steel slag. (2025). *Journal of Materials Research and Technology*.

[13] Durability assessment of ground granulated blast furnace slag-based CO_2 sequestered concrete. (2025). *Journal of Sustainable Cement-Based Materials*.

[14] Experimental investigation on the performance of ground granulated blast furnace slag and copper slag blended recycled aggregate concrete exposed to elevated temperatures. (2025). *Journal of Building Engineering*.

[15] Murty, K.S.S., Rao, G.V.R., & Adiseshu, S. (2024). *Experimental study on the effect of colloidal nano silica in self-compacting concrete containing ground granulated blast furnace slag*. Research on Engineering Structures and Materials, 10, 1467–1481.

[16] Patel, V.J., Juremalani, J., & Kumavat, H.R. (2024). *Incorporation of high-volume ground granulated slag from blast furnaces in pavement quality concrete*. Engineering, Technology & Applied Science Research, 14(4), 14888–14893.

[17] *Fresh and mechanical properties of ground granulated blast furnace slag-based concrete: A review*. (2024). Materials Today: Proceedings.

[18] Rezvaniyanzadeh, A., & Fadaee, M.J. (2023). *Effect of ground granulated blast furnace slag on the properties of hybrid-fiber-reinforced high-strength concrete under normal and high temperatures*. Structural Concrete, 24(4), 4680–4701.

[19] Juang, C.U., & Kuo, W.T. (2023). *Properties and mechanical strength analysis of concrete using fly ash, ground granulated blast furnace slag and various superplasticizers*. Buildings, 13(7), 1644.

[20] Singh, D., Gupta, R., & Kumar, S. (2022). *Performance evaluation of self-compacting concrete containing high-volume GGBFS*. Journal of Cleaner Production, 350, 131420.

[21] Wang, H., Chen, Y., & Liu, X. (2022). *Mechanical properties and hydration characteristics of GGBFS-based concrete under marine exposure*. Cement and Concrete Composites, 128, 104432.

[22] Czarnecki, S., Shariq, M., Nikoo, M., & Sadowski, Ł. (2021). *Prediction of compressive strength of cementitious composites containing GGBFS using ultrasonic pulse velocity and machine learning*. Measurement, 172, 108951.

[23] Evaluation of graded layer in ground granulated blast furnace slag-based layered concrete. (2021). Construction and Building Materials, 276, 122218.

[24] Alnahhal, W., Alengaram, U.J., & Jumaat, M.Z. (2021). *Sustainable high-strength concrete incorporating ground granulated blast furnace slag: Mechanical and durability assessment*. Sustainability, 13(7), 3824.

[25] Gong, K., & White, C.E. (2021). *Time-dependent phase quantification and local structure analysis of hydroxide-activated slag via X-ray total scattering and molecular modeling*. Cement and Concrete Research, 149, 106554.

[26] Sanjay kumar., Rakesh kumar., Amitava bandopadhyay., T. C. Alex., Ravi Kumar B., S. K. Das., &S. P. Mehrotra. (2008), "Mechanical activation of granulated blast furnace slag and itseffect on the properties and structure of Portland slag cement", *Cement and ConcreteComposites*, 30(8), pp. 679–685.

[27] Brand, A. S., & Fanijo, E. O. (2020). A review of the influence of steel furnace slag type on the properties of cementitious composites. *Applied Sciences, 10*(22), 8210.

[28] Olonade, K. A., Kadiri, M. B., & Aderemi, P. O. (2015). Performance of steel slag as fine aggregate in structural concrete. *Nigerian Journal of Technology, 34*(3), 452–458.

[29] Shi, Y., Chen, H., Wang, J., & Feng, Q. (2015). Preliminary investigation on the pozzolanic activity of superfine steel slag. *Construction and Building Materials, 82*, 227–234.

[30] Deboucha, W., Oudjit, M. N., Bouzid, A., & Belagraa, L. (2015). Effect of incorporating blast furnace slag and natural pozzolana on compressive strength and capillary water absorption of concrete. *Procedia Engineering, 108*, 254–261.

[31] Tarawneh, S. A., Gharaibeh, E. S., & Saraireh, F. M. (2014). Effect of using steel slag aggregate on mechanical properties of concrete. *American Journal of Applied Sciences, 11*(5), 700–706.

[32] Guo, X., Shi, H., & Wu, K. (2014). Effects of steel slag powder on workability and durability of concrete. *Journal of Wuhan University of Technology–Materials Science Edition, 29*(4), 733–739.

[33] Sabet Divsholi, B., Lim, D., & Teng, S. (2014). Durability properties and microstructure of ground granulated blast furnace slag cement concrete. *International Journal of Concrete Structures and Materials, 8*(2), 157–164.

[34] Wang, Q., Yang, P. Y., & Zhang, B. (2013). Influence of steel slag on the workability of concrete. *Key Engineering Materials, 539*, 235–238.

[35] Wang, Q., Yan, P. Y., & Feng, J. W. (2011). A discussion on improving hydration activity of steel slag by altering its mineral compositions. *Journal of Hazardous Materials, 186*(2–3), 1070–1075.

[36] Lizarazo-Marriaga, J., Claisse, P., & Ganjian, E. (2011). Effect of steel slag and Portland cement in the rate of hydration and strength of blast furnace slag pastes. *Journal of Materials in Civil Engineering, 23*(2), 153–160.

[37] Wang, Q., & Yan, P. Y. (2010). Hydration properties of basic oxygen furnace steel slag. *Construction and Building Materials, 24*(7), 1134–1140.

[38] Bougara, A., Kadri, E. H., & Ezziane, K. (2010). Efficiency of granulated blast furnace slag replacement of cement according to the equivalent binder concept. *Cement and Concrete Composites, 32*(3), 226–231.

[39] Ahmedzade, P., & Sengoz, B. (2009). Evaluation of steel slag coarse aggregate in hot mix asphalt concrete. *Journal of Hazardous Materials, 165*(1–3), 300–305.

[40] Alanyali, H., Col, M., Yilmaz, M., & Karagoz, S. (2009). Concrete produced by steel-making slag (basic oxygen furnace) addition in Portland cement. *Journal of the American Ceramic Society, 92*(4), 736–748.

[41] Tsakiridis, P. E., Papadimitriou, G. D., Tsivilis, S., & Koroneos, C. (2008). Utilization of steel slag for Portland cement clinker production. *Journal of Hazardous Materials, 152*(2), 805–811.

[42] Asi, I., Qasrawi, H., & Shalabi, F. I. (2007). Use of steel slag aggregate in asphalt concrete mixes. *Canadian Journal of Civil Engineering, 34*(8), 902–911.

[43] Wu, S., Xue, Y., Ye, Q., & Chen, Y. (2007). Utilization of steel slag as aggregates for stone mastic asphalt mixtures. *Building and Environment, 42*(7), 2580–2585.

[44] Kourounis, S., Tsivilis, S., Tsakiridis, P. E., Papadimitriou, G. D., & Tsibouki, Z. (2007). Properties and hydration of blended cements with steelmaking slag. *Cement and Concrete Research, 37*(6), 815–822.

[45] Oner, A., & Akyuz, S. (2007). An experimental study on optimum usage of GGBS for the compressive strength of concrete. *Cement and Concrete Composites, 29*(6), 505–514.

[46] Xue, Y., Wu, S., Hou, H., & Zha, J. (2006). Experimental investigation of basic oxygen furnace slag used as aggregate in asphalt mixture. *Journal of Hazardous Materials, 138*(2), 261–268.

[47] Shi, C. J. (2004). Steel slag—Its production, processing, characteristics, and cementitious properties. *Journal of Materials in Civil Engineering, 16*(3), 230–236.

[48] Altun, I. B., & Yilmaz, I. (2002). Study on steel furnace slags with high MgO as additive in Portland cement. *Cement and Concrete Research, 32*(8), 1247–1249.

[49] Wainwright, P. J., & Rey, N. (2000). The influence of ground granulated blast furnace slag (GGBS) additions and time delay on the bleeding of concrete. *Cement and Concrete Composites, 22*(4), 253–257.

[50] Hwang, C. L., & Lin, C. Y. (1986). Strength development of blended blast-furnace slag cement mortars. *ACI Special Publication (SP-91)*, 1323–1340.